International Journal of Geosynthetics and Ground Engineering (2024) 10:79
https://doi.org/10.1007/s40891-024-00580-0

ORIGINAL PAPER

A New Model for Evaluating the Behaviour of Swelling Soils

Uri Komornik[1] · **David Benoliel**[2]

Received: 8 November 2023 / Accepted: 12 July 2024

Abstract
In many areas around the world, there are clayey soils that have the potential to change their volume caused by the variation in their water content. Increasing or decreasing the water content caused the clayey soils to swell or shrink, respectively. This phenomenon may cause the uplifting and settlement of structures, which may lead to considerable financial damages. The estimation of swelling displacement without addressing the swelling rate have been published by several research works. This drawback leads to the development of a new model that takes into account the swelling behavior of soils with time. The model, which consists of two hyperbolic curves, was compared with swelling test results performed on soil samples taken from several locations in Israel. Data test results were used to compare the newly introduced model with other existing mathematical models found in the literature. This analysis shows that the new model represents more accurately the behavior with time of the swelling clayey soils measured in laboratory test results than the existing hyperbolic models.

Keywords Swelling · Mathematical model · Clayey-soil · Adsorption · Laboratory data

Introduction

In many areas worldwide, there are clayey soils that have the potential to change their volume due to the variation of their water content. Increasing or decreasing the water content caused the clay soils to swell or shrink, respectively. The phenomenon of swelling-shrinking may cause the uplifting and settlement of structures, which may lead to considerable financial damages. In semi-arid countries, the penetration of water can reach several meters below the ground surface and may cause vertical and horizontal pressure on the structures. The amplitude of the swelling–shrinking phenomenon depends, among other things, on the initial water contents, the liquid limit, the initial density of the clayey soils, and the type of clay. The type of clay soils may consist of several minerals such as Montmorillonite, Illite, and Kaolinite. The clay soils that contain Montmorillonite have the most potential for swelling and shrinking. Several research works have been published regarding the estimation of the swelling displacement and the developed pressure of the clayey soils without addressing the swelling rate that developed with time [1–4]. This drawback leads to the development of a new kinetic model considering the adsorption behavior of swelling clay with time when submerged in distilled water.

Existing Models of Adsorption

The use of kinetics models to describe and estimate the adsorption of a liquid into an absorbent material has been studied since the end of the nineteenth century [5]. These studies were performed in order to evaluate the ending value of the adsorption process (isotherm) and the rate and shape of the adsorption kinetic models. The submersion of clayey soils in water creates an adsorption process which causes an augmentation of soil volume. Clay soils have a layered mineralogical structure. The expansion of clayey soils is due to the attraction of negative ions present at the surface of the clay layers with positive ions of the dipolar water molecules (adsorption). That induces the penetration of water molecules between the clay mineralogical layers and thus an augmentation of the volume of the clayey soil [6, 7]. This augmentation of volume may last several weeks until

✉ David Benoliel
Davidbo@ariel.ac.il

Uri Komornik
uri_k@ariel.ac.il

[1] Geotechnical Division, Department of Civil Engineering, University of Ariel, Science Park 3, 40700000 Ariel, Israel

[2] Department of Civil Engineering, University of Ariel, Science Park 3, 40700000 Ariel, Israel

Published online: 02 September 2024

it reaches a stage of stabilization or a relatively small variation of volume with time. At this stage, the soil is almost saturated and there is extremely small additional attraction between anions present at the surface of the clay sheets and cations present in the water. The kinetics of the swelling of clayey soils include the following three stages: (i) A relatively fast rate of swelling. At this stage, water penetrates into the soil, and its water content increases relatively very rapidly. (ii) An intermediary stage when the swelling begins to stabilize, (iii) A third stage when the swelling rate is relatively very low. The following existing models of adsorption liquid on materials were first analyzed in order to develop a new model for evaluating the adsorption behavior of swelling clayey soils with time:

Pseudo-First-Order (PFO) Kinetic Model

General Formulation (Langmuir [5] and Lagergren [8])

This model is based on the following differential equation [9–17]:

$$\frac{dS(t)}{dt} = k_1(S_f - S(t)) \tag{1}$$

where $S(t)$: The swelling fraction at time t, S_f: The swelling fraction at the end of the experiment, k_1: A first-order constant or first-order swelling rate [mm^{-1}].

By integration, Eq. (1) can be written as follows:

Table 1 Characteristics of the Ariel soil specimen at the beginning and the end of the test

Geomechanical characteristics of Ariel soil	Beginning of the test	End of the test
Constant pressure, σ_c [kPa]	1	1
Total height, H_t [mm]	11.86	13.71
Swelling [%]	–	15.64
Specific gravity, G_s [–]	2.78	2.78
Unit weight, γ_t [kN/m^3]	13.43	17.03
Water content, ω [%]	4.54	53.28
Dry unit weight, γ_s [kN/m^2]	12.85	10.97
Void ratio, e [–]	1.12	1.48
Saturation, S [%]	11.29	100
Plastic limit, PL [–]	33	33
Liquid limit, LL [–]	66	66
Plasticity index, PI [–]	33	33
Clay content [%]	58	58

$$S(t) = S_f(1 - exp(-k_1 t)) \tag{2}$$

Maghrabi Model

The Maghrabi Model which uses the following equation is based on the Pseudo-First-Order Kinetic Model: [18–20]

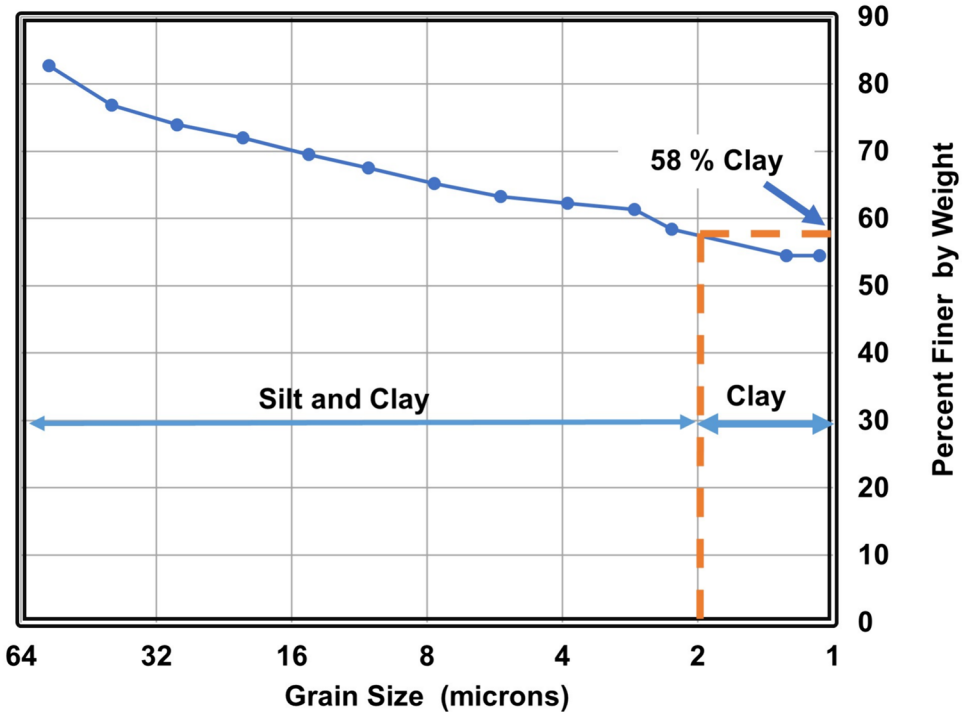

Fig. 1 Hydrometer analysis of ariel soil

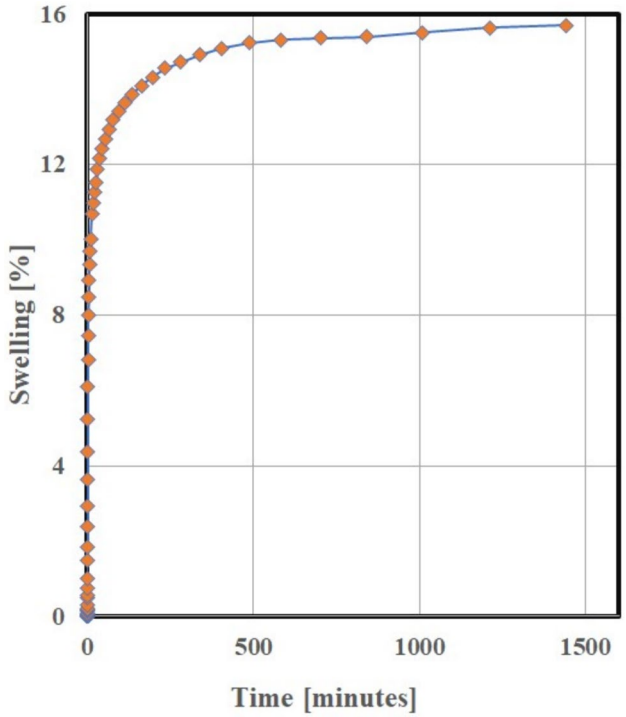

Fig. 2 Test results at constant vertical pressure of 1kPa (linear scale)

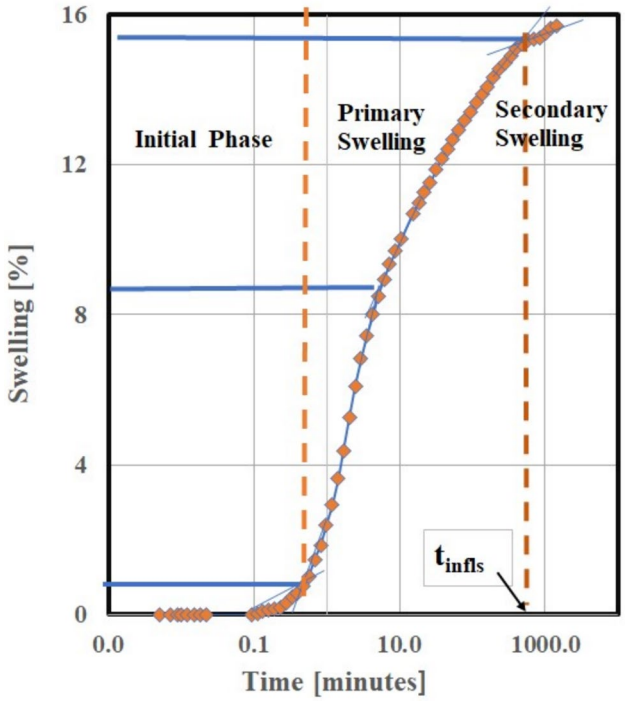

Fig. 3 Test results at constant vertical pressure of 1kPa (semi-logarithmic scale)

$$S(t) = S_f\left(1 - \frac{1}{e^{kt} + C\sqrt{t}}\right) \tag{3}$$

Where k: is a constant $[\min^{-1}]$, C: is a loss parameter $[\min^{-1/2}]$.

According to the Maghrabi Model, the parameter k is reliant on the viscosity of the water-based mud system. Maghrabi added a filtrate loss parameter denoted as C assigned to a value between zero and one.

Pseudo-Second-order (PSO) Kinetic Model

General Formulation (Blanchard et al. [18])

This model uses the following differential equation: [12–14, 16, 17, 21–25]

$$\frac{dS(t)}{dt} = k_2(S_f - S(t))^2 \tag{4}$$

where: k_2: is a pseudo-second-order constant.

By integration, Eq. (4) can be written in three different forms as follows:

$$S(t) = \frac{S_f^2 k_2 t}{1 + S_f k_2 t} = \frac{t}{\frac{1}{S_f^2 k_2} + \frac{1}{S_f}t} = \frac{S_f t}{\frac{1}{S_f k_2} + t} \tag{5}$$

The hyperbola equation (5) can be rewritten:

$$\frac{t}{S(t)} = \frac{t}{S_f} + \frac{1}{k_2 S_f^2} \tag{6}$$

Equation (6) is linear in the coordinates $t/S(t)$ versus t.

Dakshanamurthy and Peleg Model

Dakshanamurthy [26] and Peleg [27] developed the following empirical equation for estimating the swelling of clayey soils and for the adsorption of milk powder and rice, respectively, $S(t)$:

Table 2 Values of the coefficients C_1, C_2, and the intersection time of the two hyperbolae ($S_1(t)$ and $S_2(t)$) of the new model using three different methods

Method	C_1	C_2	Intersection time [min]
Adjustment	4.5	17	6.12
Least square	4.52	17.45	6.1 Computed
Substitution	4.45	17.8	6.1 Computed

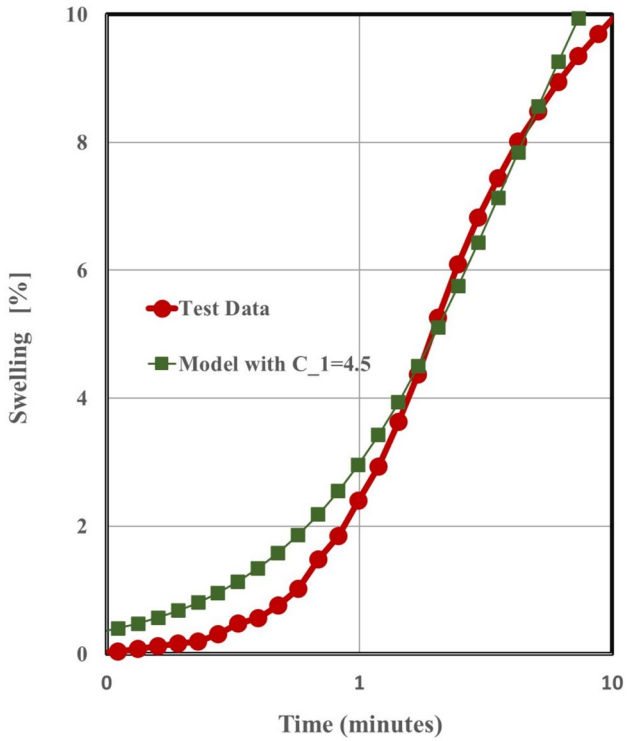

Fig. 4 Comparison between the test results and the new model using the coefficient C_1 (semi-logarithmic scale)

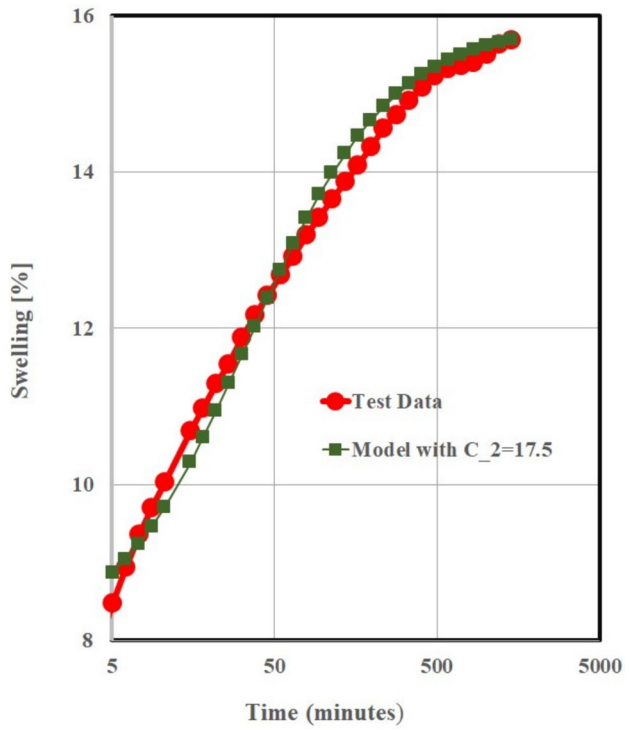

Fig. 5 Comparison between the test results and the new model using the coefficient C_2 (semi-logarithmic scale)

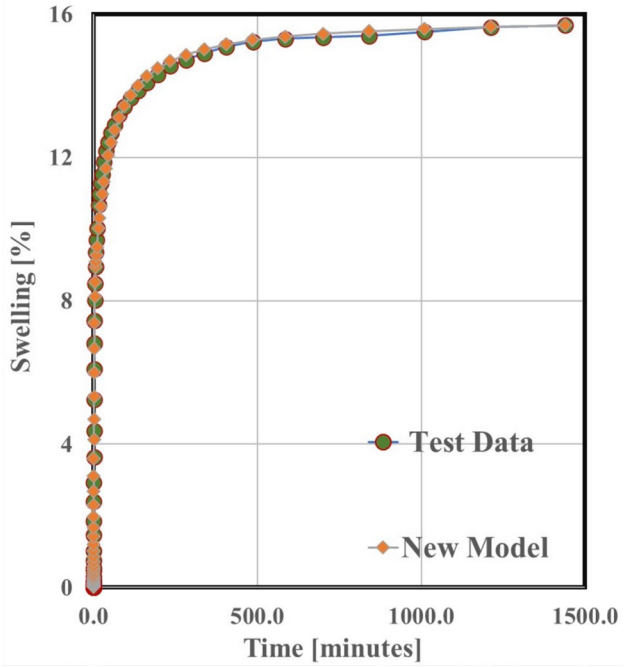

Fig. 6 Comparison between the behavior of free swelling of the test results on ariel soil and the new model (linear scale)

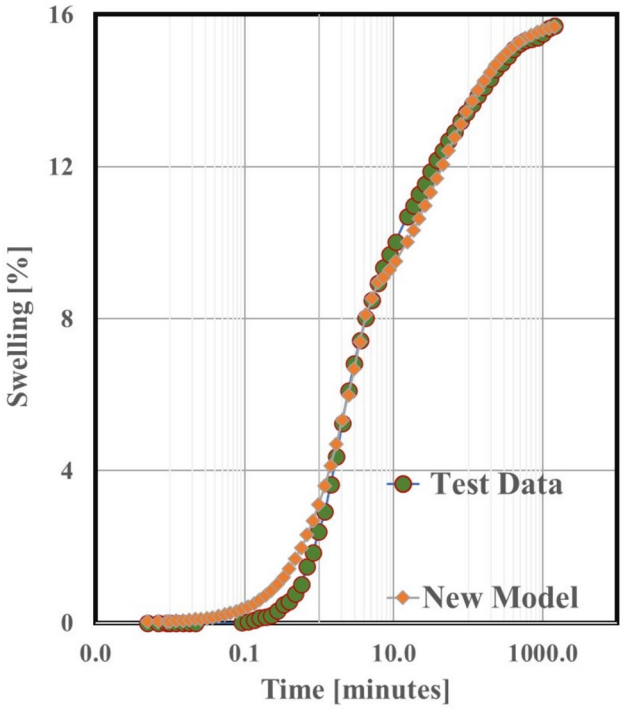

Fig. 7 Comparison between the behavior of free swelling of the test results on ariel soil and the new model (semi-logarithmic scale)

$$S(t) = \frac{t}{a + bt} \tag{7}$$

where a and b are parameters of the hyperbola. Compared to Eq. (5), coefficients a and b can be written as follows:

$$\mathrm{a} = \frac{1}{S_f^2 k_2} b = \frac{1}{S_f} \tag{8}$$

Vayssade Model

Vayssade [28] proposed the following equation for estimating the relative displacement of clayey soils $S(t)$ at time t:

$$S(t) = \frac{tS_f}{B + t} \tag{9}$$

where: B: A constant depending on the clayey soil.

In the coordinates $S(t)$ versus $S(t)/t$, Eq. (9) is linear ($S(t) = S_f - B(S(t)/t)$ and the coefficient B can be obtained by measuring the slope of this line. S_f can be obtained by extrapolation of the line $S(t)/t$ equal to zero. According to Vayssade [25] model:

$$B = t_{0.5} = t\left(\frac{1}{2}S_f\right) \tag{10}$$

where: $t_{0.5}$: The time at half stabilization swelling S_f.

Equation (9) can be written as follows:

$$S(t) = \frac{S_f t}{t_{0.5} + t} \tag{11}$$

Parcevaux Model

Parcevaux [29] proposed the following equation for estimating the swelling of clayey soils $S(t)$:

$$S(t) = G\frac{t}{B + t} \tag{12}$$

Table 3 Statistical parameters obtained from analyses for the new model and the existing models using test results on Ariel soil

Model	R^2	*RMSE*	*KS*
New model	0.995	0.4038	10.98
PSO hyperbola	0.98	0.7902	19.15
PSO Parcevaux	0.97	0.9802	47.36
PSO Vayssade	0.96	1.034	51.16
PFO Maghrabi	0.92	1.419	42.48
PFO exponential	0.68	2.995	114.69

where: G and B: Constants of the hyperbola depending on the clayey soil properties.

Equation (12) can be rewritten:

$$\frac{t}{S(t)} = \left(\frac{1}{G}t + \frac{B}{G}\right) \tag{13}$$

The parameters G and B can also be obtained by drawing the linear Eq. (12) in the coordinates $t/S(t))$ versus t. G is the inverse of the slope of the linear line and B/G is obtained when the time is equal to zero.

The parameters k_1, k, C, k_2, a and B in Eqs. (2), (3), (4), (7), (9), (12) are constants which influence the rate of the curvature of the functions mentioned above.

Development of a New Model for Evaluating the Adsorption Behaviour of Swelling Soils

Formulation of the Splitting Pseudo-Second-Order Model

The main objective of this study is to find a new model that estimates more accurately the behavior of adsorption of water in soils that cause swelling of clayey soils. One of the drawbacks of the above-mentioned models is that they do not include time-dependent parameters. Their constant parameter does not allow to estimate accurately the behavior of the swelling of soil development with time. That leads to the

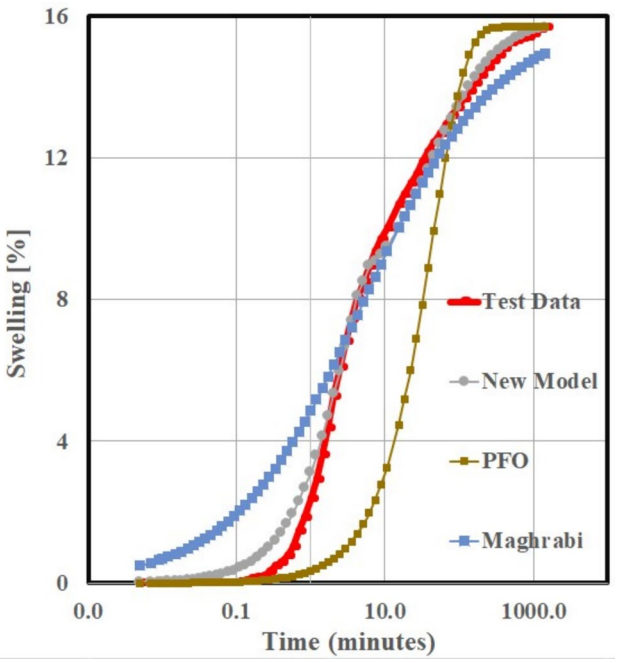

Fig. 8 Comparison between different (PFO) model analyses with test data results (semi-logarithmic scale)

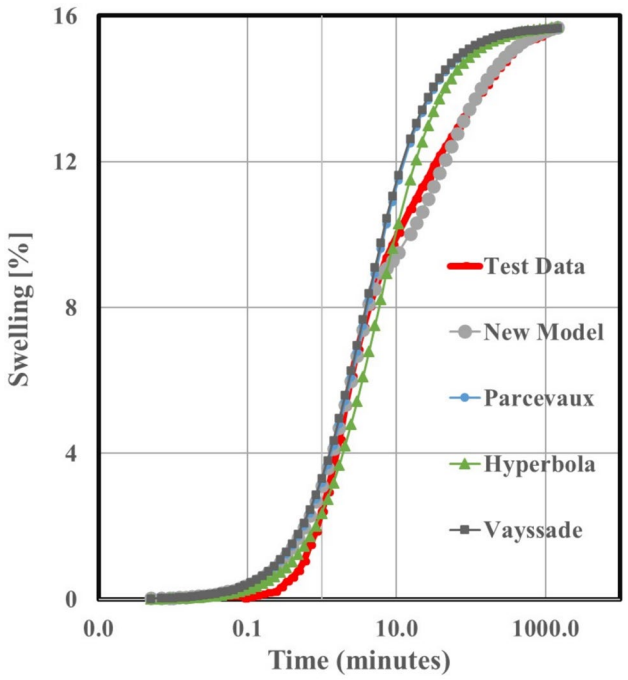

Fig. 9 Comparison between different (PSO) model analyses with test data results (semi-logarithmic scale)

development of a new empirical model that includes time-dependent parameters allowing the description of this behavior. The following new developed pseudo-second-order model equation, which includes a time-dependent rate function $C(t)$, describes the behavior of soil swelling, $S(t)$. The new model includes a hyperbolic function $C(t)$ that changes with time. This model can be written as follows:

$$S(t) = t\frac{S_f(1 + \frac{C(t_{end})}{t_{end}})}{C(t) + t} \tag{14}$$

where S_f: The stabilized swelling fraction at the end of the experiment, t_{end}: Elapsed time at the stabilization, $C(t)$: Curvature coefficient function dependent on time, $C(t_{end})$: Curvature coefficient at the end of the test.

In order to describe the adsorption behavior of the swelling process Eq. (14) is divided into two sections, which are defined by the two following equations $S_1(t)$ and $S_2(t)$. The hyperbolic function $S_1(t)$ starts at the beginning of the test until the displacement reaches a value slightly greater than $S_f/2$. The function $S_2(t)$ starts at the displacement $S_f/2$ until the swelling is stabilized at the end of the test (Appendix A).

$$S_1(t) = \frac{tS_f(1 + C_1e_c)}{C_1 + t} t \in [0, \approx t_{s_f/2}+] \tag{15}$$

and

$$S_2(t) = S_f\frac{C_2 + t(1 + C_2e_c)}{2C_2 + t} t \in [\approx t_{s_f/2}+, t_{end}] \tag{16}$$

where C_1: Curvature coefficient of the hyperbola $S_1(t)$, C_2: Curvature coefficient of the hyperbola $S_2(t)$. e_c: Ending correcting factor equals $1/t_{end}$. $t_{S_f/2}+$: Slightly greater than the time at half swelling.

Computation of C_1 and C_2

C_1 And C_2 can be evaluated by using a least-square method or by adjustment of $S_1(t)$ and $S_2(t)$ equations to the swelling test results. Another way to evaluate C_1 is by substituting $t_{S_f/2}$ (time of half swelling) into Eq. (15) (Appendix C). C_2 can also be evaluated by substituting t_{infl_s} into Eq. (16), where t_{infl_s} is the time of inflection point which defined as the beginning of the secondary swelling (Appendix C). t_{int} is the time where Eqs. (15) and (16) intersect. It can be approximately evaluated as $t_{int} \approx \frac{C_1C_2}{(C_2-C_1)}$ (Appendix B).

Table 4 Geotechnical characteristics of tested clay soils

Soil name	Water content at the beginning of the test [%]	Dry density [kN/m^3]	Type of soil	Liquid limit [%]	Plastic limit [%]	Maximum swelling using consolidometer [%]	IP [–]
Ariel clay	4.54	12.85	CH	66	33	15.64	33
Highway 6	1.64	12.38	CH	58.8	32.9	17.64	25.9
Haifa	8.74	11.65	CH	76	48.8	31.73	27.2
Montmorillonite	3.51	13.46	CH	80	44	38.91	36
Highway 4	4.52	11.74	CH	77	44.7	23.01	32.3
North Valley	4.30	13.03	CL	39	22.8	18.35	16.2
Petach Tikva	1.58	12.17	CL	41.8	23.11	18.21	18.7

CH high plasticity clay, *CL* low plasticity clay

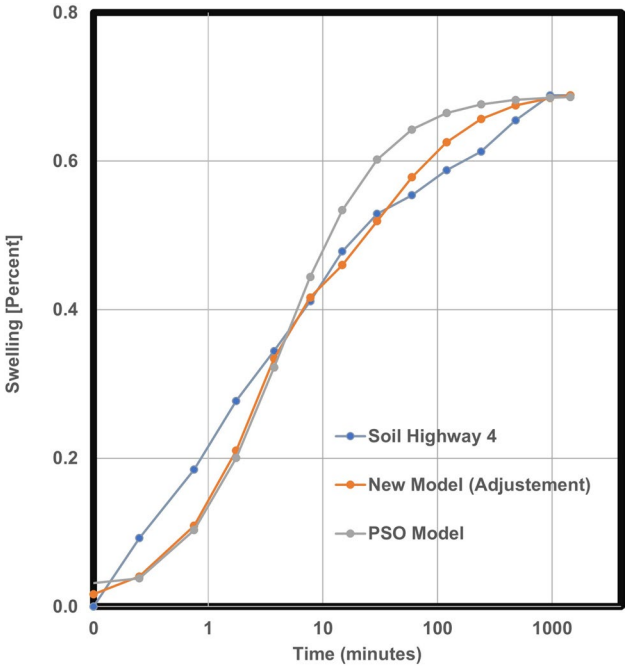

Fig. 10 Comparison between the swelling of highway 4 soil test results with the new and the existing PSO models

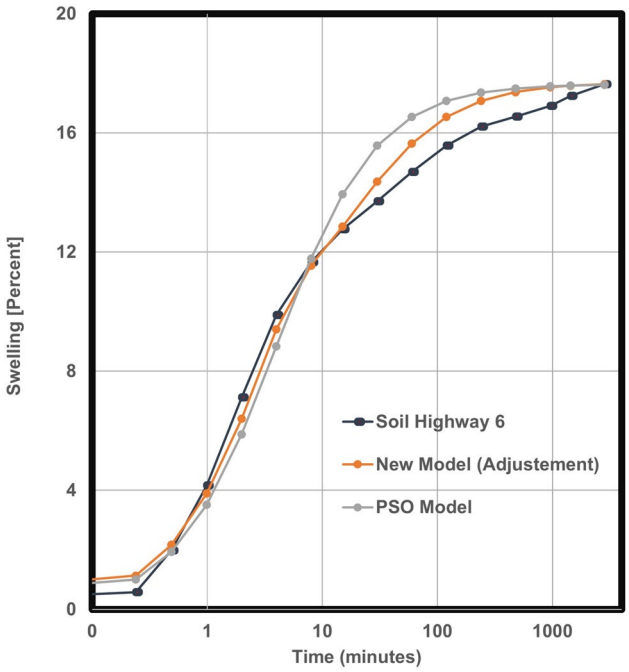

Fig. 12 Comparison between the swelling of highway 6 soil test results with the new and the existing PSO models

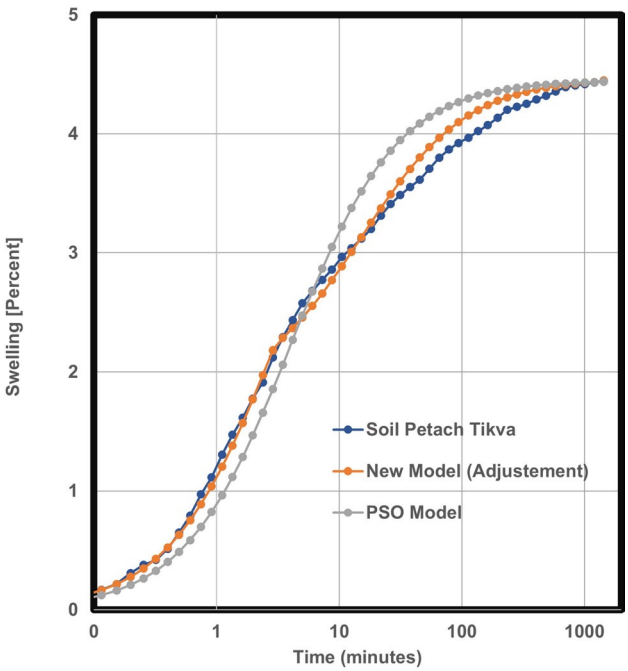

Fig. 11 Comparison between the swelling of Petach Tikva soil test results with the new and the existing PSO models

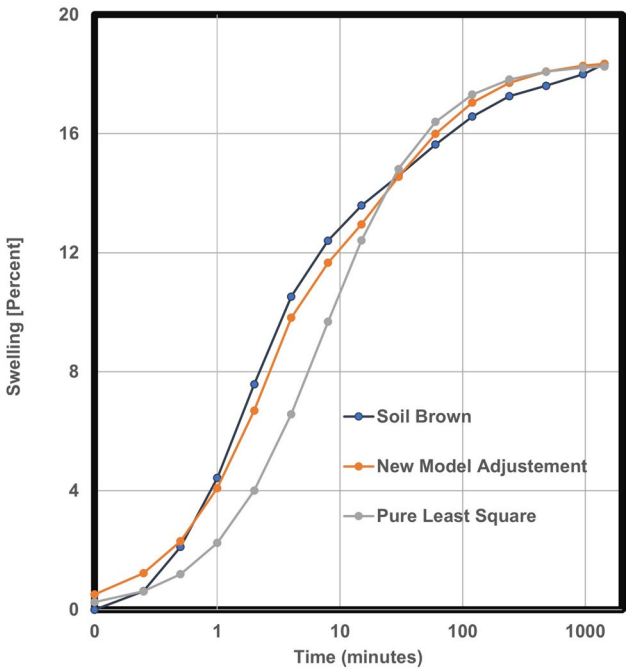

Fig. 13 Comparison between the swelling of North Valley soil test results with the new and the existing PSO models

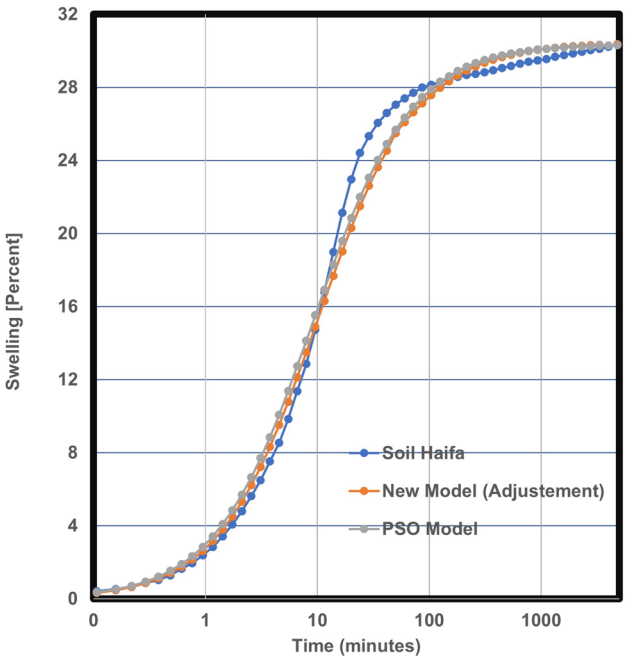

Fig. 14 Comparison between the swelling of Haifa soil test results with the new and the existing PSO models

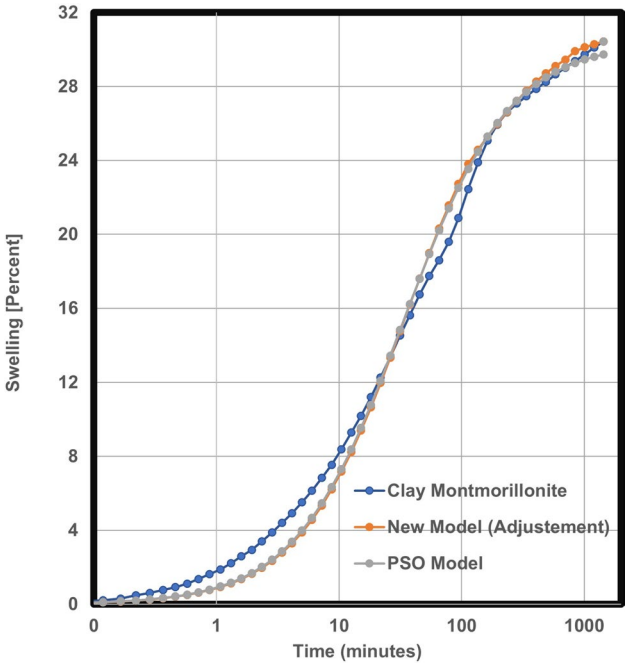

Fig. 15 Comparison between the swelling of Montmorillonite clay soil test results with the new and the existing PSO models

Table 5 Values of C_1 and C_2 parameters, intersection time (least square method), and the maximum swelling for different soils obtained for the new model

Soil	C_1	C_2	Intersection time [min]	Maximum swelling %
Highway 4	8.9	13.7	25.4	23.01
Petach Tikva	10.6	20	22.47	18.21
Highway 6	4.12	9.3	7.35	17.64
North Valley	3.9	8.2	7.25	18.35
Haifa	9.4	20.72	17.33	31.73
Montmorillonite	20.70	21.11	1068	38.91

Table 6 Values of C_1 and C_2 parameters, intersection time (adjustment method), and the maximum swelling for different soils obtained for the new model

Soil	C_1	C_2	Intersection time [min]	Maximum swelling %
Highway 4	10	20	20	23.01
Petach Tikva	10	22	6	18.21
Highway 6	3	10	4.2	17.68
North Valley	3.5	11	5.13	18.35
Haifa	10	12	60	31.73
Montmorillonite	20	22	220	38.91

Table 7 Values of B parameter (Eq. 9) for the existing PSO model obtained for several soils

Soil	B (PSO) Parameter
Highway 4	10.56
Petach Tikva	10.13
Highway 6	3.98
North Valley	7.17
Haifa	9.34
Montmorillonite	19.06

Table 8 Comparison of statistical analysis results between the new model and the existing PSO model for several soils

Soil	*RMSE* (new model)	*RMSE* (PSO model)
Highway 4	0.67	0.88
Petach Tikva	0.53	1.02
Highway 6	1.34	2.24
North Valley	1.05	3.54
Haifa	0.72	1.42
Montmorillonite	0.32	0.32

RMSE root mean square error

Test Results Performed on Clay Soils

Experiment Process for Obtaining Test Results

Swelling tests were performed according to ASTM 4546-96 [30] in order to evaluate the accuracy of the new model. Controls 26-WF31E20/SW consolidometer apparatus was used for measuring the vertical displacement. The consolidometer has two sensors, one sensor for measuring the vertical displacement and one sensor for maintaining a constant vertical pressure. A fixed constant vertical pressure of one kPa was applied to the dry sample. The initial pressure remained on the specimen until the displacement was stabilized. Petro Tech distilled water was used to submerge the soil sample in the consolidation ring. The consolidometer recorded the vertical swelling displacement of the soil sample which was developed during 24 h.

Description of the Soil Sample

The soil sample was taken from an Ariel site at a depth of 50 cm from the ground surface. The samples were classified according to ASTM D4318-17 [31] as CH (High plasticity Clay).

Preparation and Characteristics of Soil Sample

The soil sample was first washed out through a sieve ASTM # 200 (opening of 75 microns) into a large container to eliminate sand and pebbles. The large container stayed still for at least 24 h. The clear limpid water was taken out using a siphon. The mixture of silt and clay lying on the bottom was dried out in an oven at 60 °C for 3 days. The dried mixture was crushed with a cylindrical plastic hammer and passed through a sieve ASTM# 40 (opening of 425 microns) to get powder soil. The fine particles of the powder soil sample were classified according to ASTM D7928-21e1 [32]. The hydrometer analysis shows that 58% of all particles are less than 0.002 mm (Fig. 1). This dry powder soil sample was poured into the consolidometer mold of 20 cm^2 area. The upper surface was levelled using 300 g cylinder which caused 1.5 kPa pressure on the soil sample. A porous stone and a cap causing extra pressure of 0.5 kPa were laid on the top of the specimen. Table 1 shows the characteristics of the soil specimen at the beginning of the test.

Swelling Test Results

Table 1 summarizes the characteristics of the Ariel soil sample at the beginning of the test and after the swelling was stabilized at the end of the test. Figure 1 shows the Hydrometer Analysis of Ariel Soil.

Figures 2 and 3 show the test result of swelling [%] versus time [minutes] in linear and semi-logarithmic scales respectively.

The test was ended at a displacement rate of 0.003 mm per hour which was obtained after 24 h. The following observations can be derived from the test results:

1. The swelling begins after a relatively short time, about 5 s, after pouring the water into the consolidation ring.
2. The rate of swelling increases very sharply after about 5 s and stabilizes at the end of the test.
3. The moisture content of the soil sample (ω) reaches 53% at the end of the experiment.
4. The total unit weight of the soil sample (γ_t) increases during the saturation process.
5. The dry unit weight of the soil sample (γ_d) decreases during the saturation process.
6. The void ratio of the soil sample (e) significantly increases during the saturation process.
7. The three phases of swelling, initial, primary, and secondary, can be observed in the semi-logarithmic swelling graph (Fig. 3).
8. The inflection point at the primary swelling phase is relatively easily visible.
9. The primary swelling started after 30 s from the beginning of the test which is 4% of the total swelling.
10. The secondary swelling started after 406 min from the beginning of the test which is 97% of the total swelling.
11. An inflection change of rate during the primary swelling phase starts at 5 min from the beginning of the test which is 54% of the total swelling.

Comparison Between Swelling Test Results and the New Model

The coefficients C_1 and C_2 were obtained using the three methods mentioned above; least-square, adjustment, and substituting $t_{S_r/2}$ and t_{infl_s} into Eqs. (15) and (16) respectively (Table 2). Figures 4 and 5 show the relationship between the swelling versus the time for the coefficients C_1 and C_2 which were obtained using the adjustment method.

Figures 6 and 7 shows the relationship between the swelling versus the time for the test results and the new model, on a linear and semi-logarithmic scale, respectively. These figures show the good adjustment between the new model and the test results.

The adjustment of the new model and the swelling test results are evaluated using the following statistical equations:

$$RMSE = [\frac{1}{N}\sum_{i=1}^{N}(d_i - S_i)^2]^{1/2} \quad (17)$$

where $RMSE$: Root Mean Square Error, N: Number of time samples, d_i: Data at time i, S_i: Model at time i.

$$R^2 = 1 - \frac{\sum_{i=1}^{N}(d_i - S_i)^2}{\sum_{i=1}^{N}(d_i - \widehat{d})^2} \; with : \widehat{d} = \frac{1}{N}\sum_{i=1}^{N} d_i \quad (18)$$

where R^2: Root Mean Square Error, $\widehat{d}$: The average Data value.

$$KS = \max_{i=1}^{N}(|CSD_i - CSS_i|) \quad (19)$$

with:

$$CSD_i = \sum_{i=1}^{i} d_i$$
$$CSS_i = \sum_{i=1}^{i} S_i \quad (20)$$

where KS: The Kolmogorov–Smirnov parameter, CSD_i: Cumulative sum of experiment data at time i, CSS_i: The cumulative sum of model data at time i.

The criteria for adjustment evaluation of the new model to the test results for the statistical Eqs. (17), (18), and (19) are the following: The more the R^2 parameter is close to one, the better the adjustment. The more the $RMSE$ parameter is close to zero, the better the adjustment. The more the KS parameter is small, the better the adjustment. The computed parameters R^2, $RMSE$ and KS obtained for the new model are 0.995, 0.4038, and 10.98 respectively (Table 3). These parameters show a good agreement between the suggested new model and the swelling test results on Ariel soil.

Comparison Between Swelling Test Results, the New Model, and the Existing Swelling Models

Figures 8 and 9 shows the comparison between the swelling test results for the Ariel soil and the swelling behavior obtained using different models. It can seen that the best agreement between the test results is for the new suggested model. The statistical parameters calculated for the different models using Eqs. (17), (18), and (19) show that the new presented model has the best adjustment with the swelling test results (Table 3).

Application of the New Model for Different Clayey Soils

The new model was applied to estimate the swelling behavior of six different types of clayey soils. Table 4 summarizes the characteristics of these soils obtained by tests performed according to the ASTM as described above. The tests were performed according to the process described in paragraph [4.3]. Figures 10, 11, 12, 13, 14, and 15 show the results of the analyses using the new suggested model and the existing PSO models. Tables 5 and 6 show the C_1 and C_2 parameters (Eqs. 15 and 16) obtained for the new model and Table 7 shows B parameters (Eq. 9) obtained for the PSO model. According to these analyses, it can be deduced that the new proposed model estimates more accurately the behavior of the swelling soils than the existing PSO model (Table 8).

Conclusions

1. The statistical analysis shows that the new proposed model can estimate in a relatively accurate manner, the behavior of swelling clayey soils caused by changing their water contents.
2. The new introduced swelling model allows estimating the behavior of the swelling process of clayey soils during the laboratory test more accurately than the estimation obtained using the existing PSO models.
3. The statistical analyses show that the new proposed model can estimate, in a relatively accurate manner, the swelling behavior of the clayey soils tested in this research work.

Appendix A

Demonstration of Eq. (16) from Eq. (14)

$$S(t) = t\frac{S_f(1 + \frac{C(t_{end})}{t_{end}})}{C(t) + t} \quad (A1)$$

Assumptions:

$$C_2 = C(t_{end})$$

$$C(t) = \frac{C_2 t}{C_2 + t}$$

$$e_c = \frac{1}{t_{end}}$$

$$C_2(1 + e_c) \approx C_2$$

Equation (14) becomes Eq. (16):

$$S(t) = S_f \frac{(C_2 + t(1 + C_2 e_c))}{2C_2 + t} \tag{A2}$$

with:

$$S(0) = \frac{S_f}{2}$$

$$S(t_{end}) = S_f$$

Appendix B

Demonstration of $t_{int} \approx \frac{C_1 C_2}{C_2 - C_1)}$

Equating Eq. (15) to (16):

$$S_1(t) = S_2(t) \tag{B1}$$

Approximations:

$$C_1 e_c \approx C_2 e_c \approx 0$$

$$\frac{t}{C_1 + t} \approx \frac{C_2 + t}{2C_2 + t}$$

Time of intersection of the two curves:

$$t_{int} \approx \frac{C_1 C_2}{C_2 - C_1} \tag{B2}$$

Appendix C

Computation of C_1 and C_2 by Substitution

From Eq. (15):

$$S_1(t) = \frac{t S_f (1 + C_1 e_c)}{C_1 + t} \tag{C1}$$

$$S_1(t_{s_f/2}) = \frac{S_f}{2}$$

where $t_{s_f/2}$ the time when half the swelling occurs.

$$\frac{S_f}{2} = \frac{t_{s_f/2} S_f (1 + C_1 e_c)}{C_1 + t_{s_f/2}}$$

Approximations:

$$C_1 e_c \approx 0$$

C_1 can be expressed:

$$C_1 \approx t_{s_f/2} \tag{C2}$$

From Eq. (16):

$$S_2(t) = S_f \frac{C_2 + t\left(1 + C_2 e_c\right)}{2C_2 + t} \tag{C3}$$

Observe the time and the swelling at the secondary swelling inflection: t_{infl_s} and $S_2(t_{infl_s})$ (Fig. 3). The Eq. (16) becomes:

$$S_2(t_{infl_s}) = S_f \frac{(C_2 + t_{infl_s}(1 + C_2 e_c)}{2C_2 + t_{infl_s}}$$

Approximations:

$$C_2 e_c \approx 0$$

$$C_2 \approx t_{infl_s} \frac{S_f - S_2(t_{infl_s})}{2S_2(t_{infl_s}) - S_f} \tag{C4}$$

Author Contributions All the authors contributed to the study and developed the new model.

Funding Open access funding provided by Ariel University.

Data Availability The Data that support the findings of this study are available from the corresponding author D.S. Benoliel, e-mail: Davidbo@ariel.ac.il or from the following Link: \Users\Davidbo\OneDrive-ariel.ac.il\Data_Clay\textbackslashhttpsarielacil-my.sharepoint.comxgpersonaldavidbo_ariel_ac_ilEXeDDILdj2tKhuarktjP9VcBGYuZAKuvmulMIYC4gCImige=fvGAxz.

References

1. David D, Komornik A, Goldberg M (1973) Swelling and bearing characteristics in clayey sands and loess. In: Proceeding of the

eight international conference on soil mechanics and foundation engineering, Moscow, 1973
2. Djedid A, Ouadah N (2013) Indirect estimation of swelling clay soils parameters. EDGE 18
3. Mowafy Y, Bauer G (1985) Prediction of swelling pressure and factors affecting the swell behaviour of an expansive soil. Transp Res Rec 1032:23–28
4. Nayak N, Christensen R (1971) Swelling characteristics of compacted, expansive soils. Clays Clay Miner 19:251–261. https://doi.org/10.1346/CCMN.1971.0190406
5. Langmiur I (1918) The adsorption of gases on plane surfaces of glass, mica and platinum. J Am Chem Soc 40:1361–1403. https://doi.org/10.1021/ja02242a004
6. Das B, Sobhan K (2017) Principles of geotechnical engineering, 9th edn. Cengage Learning, Boston
7. Fritz T, Muller-Vonmoos M (1989) The swelling behaviour of clays. Appl Clay Sci 4:143–156. https://doi.org/10.1016/0169-1317(89)90005-7
8. Lagergren I (1898) About a theory of the so-called adsorption of soluble substances. K Sven Vetenskapsakad Handl 24:1–39
9. Ahmed L, Atif R, Eldeen T, Yahya I, Omara A, Eltayeb M (2019) Study the using of nanoparticles as drug delivery system based on mathematical models for controlled release. Int J Latest Technol Eng Manag Appl Sci 5:52–56
10. Azizian S (2004) Kinetic models of sorption: a theoretical analysis. J Colloid Interface Sci 276:47–52. https://doi.org/10.1016/j.jcis.2004.03.048
11. Eltayeb M, Stride E, Ediridinghe M, Harker A (2016) Electrosprayed nanoparticule delivery system for controlled release. Mater Sci Eng C 66:138–146. https://doi.org/10.1016/j.msec.2016.04.001
12. Eris S, Azizian S (2017) Extension of classical adsorption rate equations using mass of adsorbent: a graphical analysis. Sep Purif Technol 179:304–308. https://doi.org/10.1016/j.seppur.2017.02.021
13. Hu Q, Wang Q, Feng C, Zhang Z, Lei Z, Shimuzu K (2018) Insights into mathematical characteristics of adsorption models and physical meaning of corresponding parameters. J Mol Liq 254:20–25. https://doi.org/10.1016/j.molliq.2018.01.073
14. Lalji S, Ali S, Ahmed R, Hashmi S, Awan Z (2021) Comparative performance analysis of different swelling kinetic models for evaluation of shale swelling. J Pet Explor Product Technol. https://doi.org/10.1007/s13202-021-01387-9
15. Simonin J (2016) On the comparison of pseudo-first order and pseudo-second order rate laws in the modelling of adsorption kinetics. Chem Eng J 300:254–263. https://doi.org/10.1016/j.cej.2016.04.079
16. Largitte L, Pasquier R (2016) A review of the kinetics adsorption models and their application to the adsorption of lead by an activated carbon. Chem Eng Res Des 109:495–501. https://doi.org/10.1016/j.cherd.2016.02.006
17. Yousef R, Qiblawey H, El-Naas M (2020) Adsorption as a process for produced water treatment: a review. Process 8:1657
18. Lalji S, Ali S, Awan ZUH, Jawed Y (2021) A novel technique for the modelling of shale swelling behaviour in water-based drilling fluids. J Pet Explor Product Technol 11:3421–3435. https://doi.org/10.1007/s13202-021-01236-9
19. Lalji S, Ali S, Awan Z, Jawed Y, Tirmizi S, Louis C (2022) Development of modified scaling swelling model for the prediction of shale swelling. Arab J Geosci 15:353. https://doi.org/10.1007/s12517-022-09607-0
20. Tariq Z, Murtaza M, Mahmoid M, Aljawad M, Kamal M (2022) Machine learning approach to predict the dynamic linear swelling of shales treated with different water based drilling fluids. Fuel. https://doi.org/10.1016/j.fuel.2022.123282
21. Blanchard G, Maunaye M, Martin G (1984) Removal of heavy metals from waters by means of natural zeolites. Water Res 12:1501–1507. https://doi.org/10.1016/0043-1354(84)90124-6
22. Guo X, Wang J (2019) A general kinetic model for adsorption: theoretical analysis. J Mol Liq. https://doi.org/10.1016/j.molliq.2019.111100
23. Ho Y (2006) Review of second-order models for adsorption systems. J Hazard Mater B 136:681–689. https://doi.org/10.1016/j.jhazmat.2005.12.043
24. Ho Y, McKay G (1999) Pseudo-second order model for sorption process. Process Biochem 34:451–465. https://doi.org/10.1016/S0032-9592(98)00112-5
25. Liu Y, Shen L (2008) From Langmuir kinetics to first- and second-order rate equations for adsorption. Langmuir 24:11625–11630. https://doi.org/10.1021/la801839b
26. Dakshanamurthy V (1978) a new method to predict swelling using a hyperbolic equation. Geotech Eng 9:29–38
27. Peleg M (1998) An empirical model for description of moisture sorption curves. J Food Sci 53(4):1216–1220
28. Vayssade B (1978) Contribution à l'Etude du Gonflement Interparticulaire des Sols Argileux. Dissertation, Ecole Nationale Supérieure des Mines de Paris
29. Parcevaux P (1980) Etude Microscopique et Macroscopique du Gonflement des Sols Argileux. Dissertation, Université Pierre et Marie Curie, Paris
30. ASTM D4546-08 (2008) Standard-based model for swell characterisation of expansive clays
31. ASTM-4318-17 (2017) Liquid limit, plastic limit, and plasticity index of soils
32. ASTM-7928 (2007) Particle-size distribution (gradation) of fine-grained soils using the sedimentation (hydrometer) analysis